International Journal of Current Advanced Research
ISSN: O: 2319-6475, ISSN: P: 2319-6505, Impact Factor: 6.614
Available Online at www.journalijcar.org
Volume 8; Issue 03 (A); March 2019; Page No. 17606-17611
DOI: http://dx.doi.org/10.24327/ijcar.2019. 17612.3345

Research Article

SYNTHESIS OF METAL AND NONMETAL CO-DOPED TIO2 NANO MATERIAL FOR THE IMPROVED PHOTOCATALYTIC AND ANTIBACTERIAL ACTIVITY STUDIES

Divya Lakshmi K V and Siva Rao T*

Department of Inorganic and Analytical Chemistry, Andhra University, Visakhapatnam 530003, India

A R T I C L E I N F O

Article History:
Received 6th December,, 2018
Received in revised form 15th January, 2019
Accepted 12th February, 2019
Published online 28th March, 2019

Key words:
TiO2; Mn-S; Sol-gel method; Xylenol orange; antibacterial activity; Photocatalyitc activity

A B S T R A C T

The present study explained the Photocatalytic and antibacterial activity of mesoporous Mn-S co-doped TiO2 nano material synthesized by using sol-gel method. As prepared samples were characterized by XRD, SEM-EDX, FT-IR, UV-Vis-DRS, TEM and BET. These Characterization and experimental results revealed that there is a formation of anatase phase, presence of co-doped ions and their oxidation states, spherical with smooth surface morphology, frequency shift of Ti-O-Ti in co-doped TiO2 due to substitutional doping of Mn and S into TiO2 lattice, decreased band gap energy and particle size, increased in surface area. The efficiency of photocatalytic and antibacterial activity was evaluated by degradation of Xylenol orange (XO) and Sphingomonas paucimobilis (MTCC-6363) respectively. The complete degradation of XO was achieved in 120 min.

INTRODUCTION

Now a day's most of the organic pollutants introduced in to the water system from various sources like Industrial effluents, textile industries, and agricultural runoff chemical spills [1-3]. These pollutants present in the environment are highly persistent in nature and causes of much concern to the societies and regulation authorities around the world. Xylenol Orange is a dye extensively used in textile industries [4-5] also used as indicator it causes environmental pollution. Polluted water contains several pathogenic bacteria and fungi. *Sphingomonas paucimobilis* (MTCC-6363) are gram negative bacteria which cause leg ulcers on human body [6-7]. The present study tells about decontamination process and remediation of dyes and pathogenic bacteria from contaminated water. TiO_2 is a semiconductor material widely used in photocatalytic reactions [8-9] due to its photo stability, non toxicity, and reusability and comparatively inexpensive. The main drawback of TiO_2 is its large bandgap energy (3.2eV) [10-12] and high recombination rate of photo generated charge carriers because TiO_2 excited only in UV-light so its lead to low quantum efficiency. Therefore the modifications to Titania have great attention and some methods were investigated to increase the visible light photoactivity by doping with various metal and non-metal elements [13-15]. According to previous studies co-doped TiO_2 with metal and non-metal elements can improve the photocatalytic performance when compared to single doped TiO_2.

Corresponding author:* **Divya Lakshmi K V
Department of Inorganic and Analytical Chemistry, Andhra University, Visakhapatnam

Among all the transition metals Manganese is preferred because the presence of t 2g orbital of d is very close to valance band by which the absorption shifts to visible region [16]. Various non-metal elements have been used to improve the photocatalytic activity of TiO_2 under visible light and the advantage of non metal doping is to minimize the recombination centres. Sulfur is preferred because it replaces some Ti^{4+} ions in TiO_2 lattice[17]. Hence we have selected Mn and S as dopants to synthesize co-doped TiO_2 using sol-gel method. The main advantage of this method in preparing catalytic material having excellent control over the properties of the product via host of parameters that are accessible aging, good homogeneity, control grain size, drying and heat treatment [18-19].

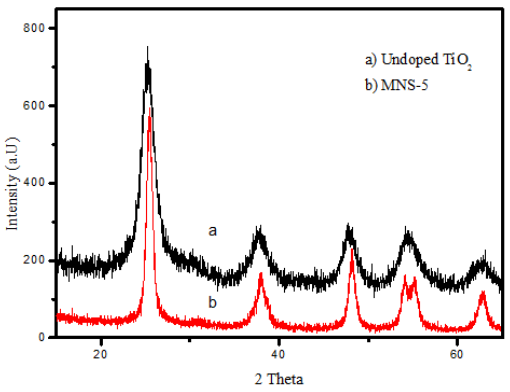

Fig 1 The XRD pattern of the synthesized undoped and co-doped TiO_2 with different wt% of Mn2p and S2p.

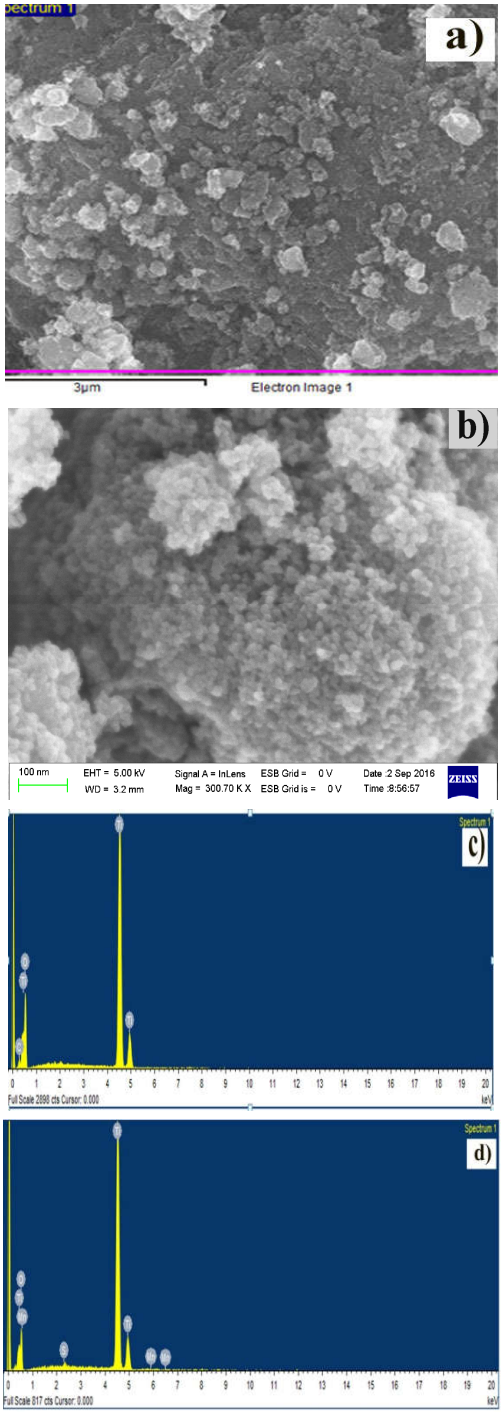

Fig 2 The SEM images of a) undoped TiO_2 b) MNS-5 and the EDS spectrum of c) undoped TiO_2 and d) MNS-5.

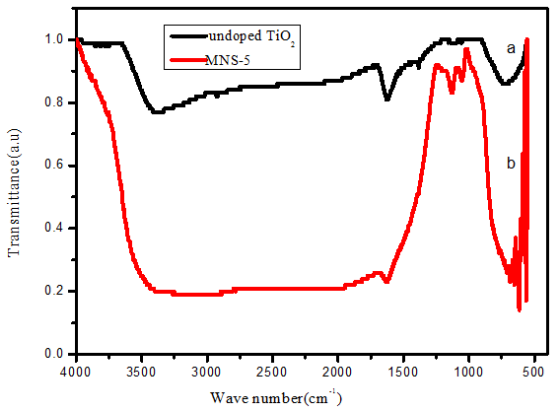

Fig 3 The FT-IR spectrum of a) Undoped TiO_2 b) MNS-5

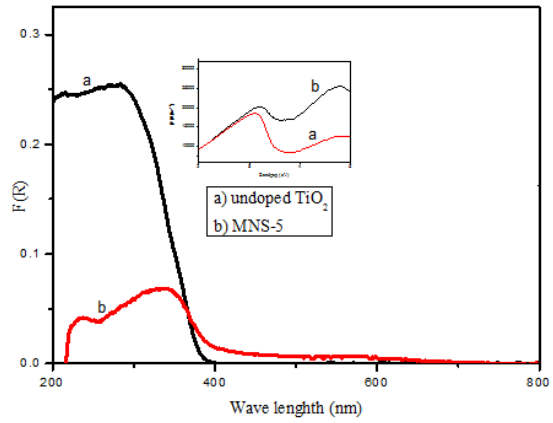

Fig 4 Plots of transformed Kubelka-Munk $[F(R).h\nu]^{\wedge 2}$ versus hν for different Percentage of co-doped TiO2, undoped TiO2

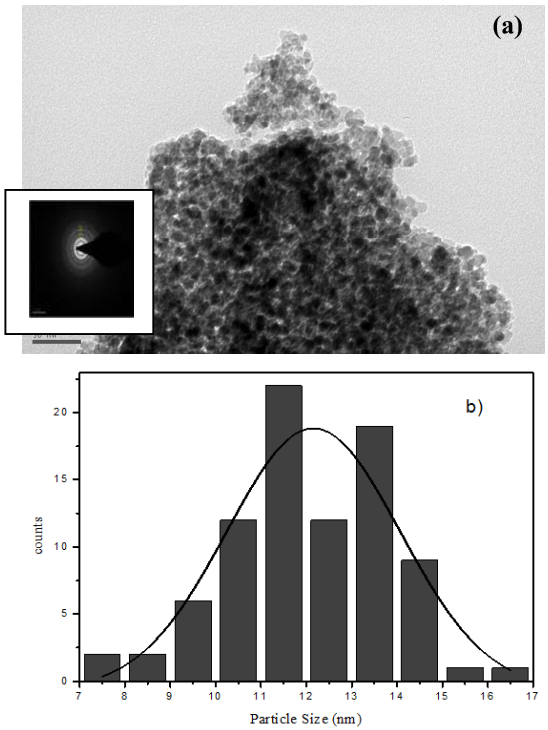

Fig 5 The TEM images of a) MNS-5 with SAED pattern of co-doped TiO_2 b) histogram and Gussian fitting of MNS-5.

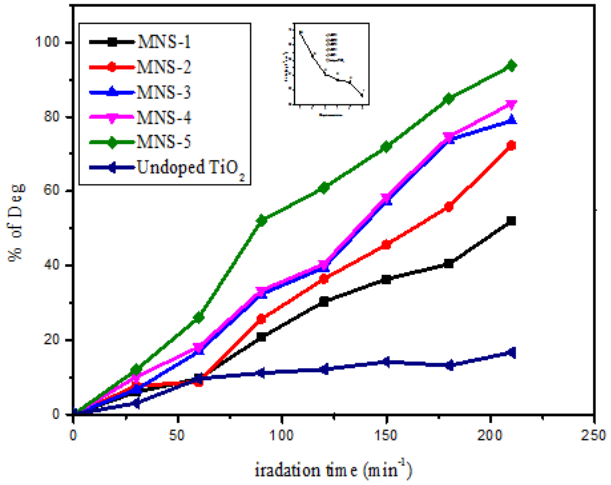

Fig 6 Effect of dopant concentration on photocatalytic of co-doped titania for rate of degradation of XO dye. Here, catalyst dosage 100 mg/L , pH 3 and XO= 10 ppm.

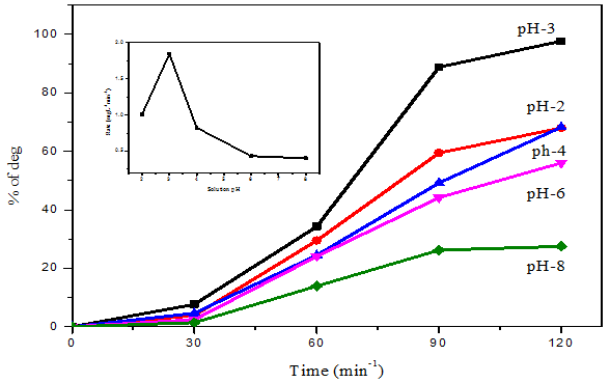

Fig 7 The effect of pH on the rate of degradation of XO dye by Mn 2p & S 2p co-doped TiO_2 Here, catalyst dosage 100 mg/L and XO= 10 ppm.

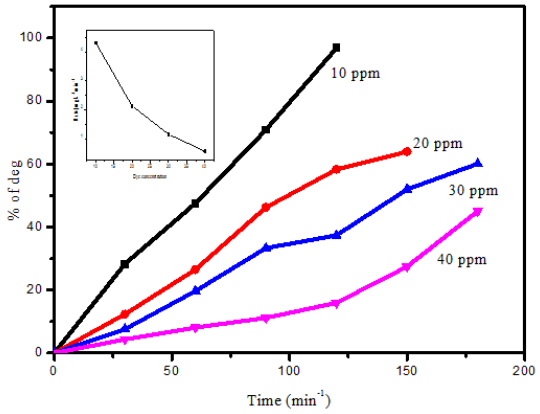

Fig 8 Effect of catalyst dosage on the degradation of XO by MNS-5 co-doped TiO_2 here pH = 3 and XO=10 ppm

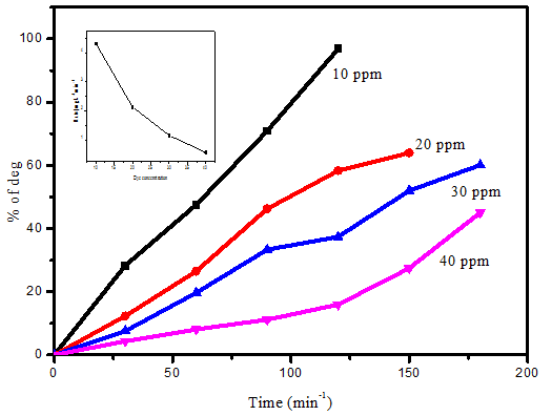

Fig 9 Effect of initial concentration of the dye on the rate of degradation of XO dye Here, pH=3 and catalyst dosage-100 mg/L.

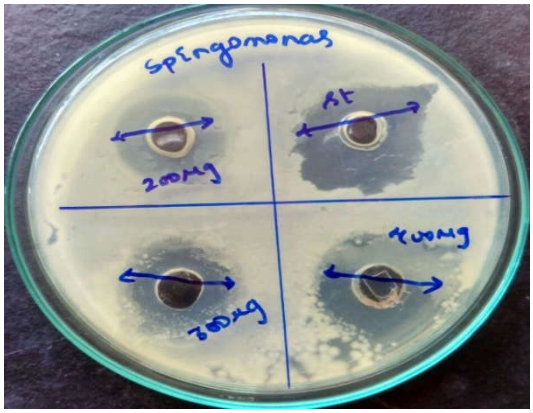

Fig 10 Zone of inhibition of *Sphingomonas paucimobilis* (MTCC-6363)

Table 1 The Results of crystallite size (XRD), Band gap (UV-ViS-DRS) &BET surface area.

S.No	Catalyst code no	Crystallite size (nm)	Band gap Energy (eV)	BET surface area analysis		
				Surface area (m^2/g)	Pore Volume (Cm^3/g)	Pore Size (nm)
1	MNS-5	3.03	2.5	155.8786	0.2095	4.8
2	Un doped TiO_2	13.3	3.2	76.3687	0.2153	10.3

Table 2 Agar-well diffusion of co-doped TiO_2 nano particles (MNS-5) *Sphingomonas paucimobilis* (MTCC-6363)

S.no	Catalyst	Organism	200µg/mL	300µg/mL	400µg/mL	Standard (Chloramphenicol) 100µg/mL
1	MNS-5	*Sphingomonas paucimobilis* (MTCC-6363)	15	16	18	18

Experimental

Materials

All the Chemicals used in the synthesis process were reagent grade and the solutions were prepared with double distilled water without further purification. N-butyl tetra ortho titanate ($Ti(OBu)_4$), Manganese nitrate $[Mn(NO_3)_2].6H_2O$ and Thiourea are obtained from E-Merck (Germany) were used as a precursors of titanium, manganese, sulfur for preparing undoped TiO_2 and co-doped TiO_2 catalysts respectively. Xylenol orange dye pollutant obtained from high media, India.

Preparation of Mn and S co-doped Titania Nano Materials

Manganese and sulphur co-doped (MNS-5) (1.0 Wt % Mn-0.25 Wt % S) nano Titania was synthesized by using sol-gel method. In this process n-Butyl ortho titanate (20 mL) was added in ethanol and acidified with Nitric acid (3.2 mL) taken in a beaker (solution-I) and stirred for 15min. In another beaker Manganese Nitrate and Thiourea, precursors of Mn and S were dissolved in ethanol and added deionised water (7.2 mL) for the purpose of hydrolysis process (solution-II). Then solution-II was added to solution-I drop wise under vigorous stirring. After complete addition of solution (II), a colloidal suspension formed was continued to stir for 90 min and aged for 48 h. The obtained gel was dried in an oven at 70 ^oC and it was well ground and calcined at 450 ^oC for about 5 h in a muffle furnace. Finally it was cooled and ground to form homogeneous powder. For preparation of undoped TiO_2 the same procedure followed without addition of sulfur and manganese precursors.

Characterization of Catalyst

The crystalline structure of photocatalyst were determined by powder X-ray diffraction (XRD) spectra taken (model ultima IV) Rigaku) using anode Cu-WL 1 (λ=1.5406 nm) radiation with a nickel filter. The applied current and voltage were 40 mA and 40 kV respectively. The average crystallite size of anatase was determined according to the Scherrer equation using (FWHM) data of the selected peak. The surface area and porosity measurements were carried out with a micrometrics Gemini VII surface area analyzer. The Nitrogen adsorption/desorption isotherms were recorded 2-3 times to obtain reproducible results and reported by BJH surface/volume meso pore analysis. The micro pore volume was calculated using the Frenkel-Halsey-Hill isotherm

equation. Each sample was degassed at 300 ^{o}C for 2 h. The size and shape of the nano particles were recorded with TEM measurements using JEOL/JEM 2100, operated at 200 kV. The morphology and elemental composition of the catalyst was characterized using scanning electron microscope (SEM) (ZEISS-SUPRA 55 VP) equipped with an energy dispersive X-ray (EDS) spectrophotometer and operated at 20 kV. FT-IR spectra of the samples were recorded on a FT-IR spectrometer (Nicolet Avatar360). The Diffuse reflectance spectra (DRS) were recorded with a Shimadzu 3600 UV-Visible- NIR Spectrophotometer equipped with an integrating sphere diffuse reflectance accessory, using $BaSO_4$ as reference scatter. Powder samples were loaded into a quartz cell and spectra were recorded in the range of 200-900 nm. The extent of XO degradation was monitored using UV-Vis spectrophotometer (Shimadzu 1601).

Photo Catalytic activity of the Catalyst-Degradation of Xylenol Orange dye

The photocatalytic efficiency of the synthesized catalyst, Mn and S co-doped (MNS-5) nano titania was carried out by degradation of XO dye under visible light irradiation in the photocatalytic reactor A high pressure 400 W (35,000 lm) mercury vapour lamp with UV filer (Oriel, 51472) was used as a visible light irradiation source. The degradation procedure was performed by taking 100 mL of XO dye solution of required concentration (1-10 mgL^{-1}) containing sufficient amount of the catalyst in a 150 mL Pyrex glass vessel under continuous stirring placed about 20 cm away from the light source. The running water was circulated around the sample container to filter IR radiation to maintain constant solution temperature in a pyrex glass reaction vessel. The solution was stirred in dark for 30min to attain adsorption – desorption equilibrium of XO dye on the catalyst surface. After visible light illumination small aliquots of sample were collected from the reaction mixture using Millipore syringe (0.45µm) at different intervals of time to observe the change in XO dye concentration by measuring the absorbance at 446 nm using UV-visible (Milton Roy Spectronic 1201) Spectrophotometer. A pH meter (Elico Digital pH meter model 111E, EI) was used for adjusting and investigation of pH variation during the degradation process. The pH of the dye solutions was adjusted prior to irradiation by addition of 0.1 N NaOH / 0.1 N HCl to get required pH. The percent of degradation of XO dye was calculated from the following equation.

$$\% \text{ of degradation} = A_o - A_t / A_o \times 100$$

Where, A_o is initial absorbance of dye solution before degradation and A_t is absorbance of dye solution at time t.

The optimum reaction conditions are attained by varying the reaction parameters, such as dopant concentration, effect of pH, catalyst dosage and initial dye concentration and results are discussed in section 4.1-4.4.

Antibacterial Activity study of Photocatalyst

Antibacterial activity study of MNS-5 was carried out by Agar-well diffusion method against bacterial strain namely *Sphingomonas paucimobilis* (MTCC- 6363) of Gram *–ve* bacteria. Nutrient Agar (High media- india) dissolved in water was distributed in 100 mL conical flask and sterilized in an autoclave at 121^{o}C 15lbp for 15 min. After autoclaved the media, poured sterilized petri plates were prepared and swabbed using L-shaped glass rod with 100 µL of 24 h mature broth culture of bacterial strain. The wells were made by sterile cork-borer. Wells are created in the petri plates and different concentrations of TiO_2 co-doped (MNS-5) nano particles are injected (200 µg/mL/ 300 µg/mL/ 400 µg/mL). The TiO_2 nano particles were dispersed in sterile water and it was used as a negative control and simultaneously the standard Antibiotic Chloramphenicol (100 µg/mL) as positive control were tested against the bacterial pathogen, then the plates were incubated 24 h at 37 ^{o}C. In the zone Inhibition of every well measured in millimetre.

Characterizations

X-Ray Diffraction Studies (XRD)

Figure.1 shows the X-ray diffraction patterns of undoped and co-doped TiO_2 nano catalysts. The synthesized samples are in anatase phase. The characteristic highest intensity peak observed at $2\theta=25.5^0$ along with 2θ at 37.9^{o}, 48.4^{o}, 54.8^{o} which can be indexed to the (101), (004), (200) and (211) planes of anatase TiO_2 (JCPDS card no. 21- 1272). No extra peaks were observed due to doping of Mn and S. The average crystallite sizes of undoped and co-doped TiO_2 catalysts were determined by Debye-Scherer equation and co-doped sample crystallite size obtained from 3.03 nm compared to undoped TiO_2 13.3 nm and the values are given in Table.1 from this table concluded that MNS-5 having less crystallite size compared to undoped TiO_2. This is may be due to increase in the metal dopant concentration suppresses the crystal growth leads to decrease in crystallite size [20-21].

$$D = K\lambda/\beta \cos\theta$$

Scanning electron Microscopy - Energy dispersive X-ray Spectroscopy (SEM-EDX)

The SEM images of undoped and co-doped TiO_2 (MNS-5) catalysts are shown in Fig.3. It can be seen that the MNS-5 exhibit eclectic morphology compared to undoped TiO_2.The SEM images of undoped TiO_2 shows spherical shaped agglomerated particles with uneven size distribution (Fig.2a). However, MNS-5 shown less agglomerated spherical shaped particles with decreased particle size (Fig.2b). From the SEM results it can be concluded that agglomeration and particle size are decreased greatly in MNS-5 due to co-doping of Mn and S into TiO_2 lattice and their constituent elements presence was confirmed by EDX (Fig.2d) analysis.

Fourier Transform –Infra Red Spectroscopy (FT-IR)

The FT-IR spectra of synthesized Co-doped nano catalyst showed a strong absorption band at 3441.48 cm-1 and narrow band at 1620.27 cm^{-1} due to the stretching and bending vibrations of the OH present on the surface of TiO_2 catalyst (Fig.3) which is in good agreement with the previous studies [22]. The appearance of representative peaks for S=O stretching mode, Mn-O and Ti–S stretching vibration were assigned to 1400.61, 601.1cm^{-1} and 1051.60cm^{-1} respectively as compared with FT-IR spectra of undoped TiO_2 . A low frequency strong band seen at 400-900 cm-1 corresponds to O-Ti-O vibration mode [23-24]. Hence, FT-IR study confirmed that Mn and S are substitutionally doped in to TiO_2 lattice by replacing Ti^{4+} ions respectively.

Ultraviolet-Visible Diffuse Reflectance Spectroscopic Studies (UV-Vis-DRS)

The diffused reflectance spectral (DRS) data showed that the synthesized undoped and co-doped (MNS-5) samples had profound effect on its optical response in the visible wavelength range. Bandgap of synthesized samples were calculated by using the formula (Eg=1240/λ), Where Eg is bandgap and λ is wave length. Further it was supported by the calculated band gap energies of the synthesized samples from the reflectance spectra using the Kubelka-Monk formalism and Tauc plot method [25] shown in Fig. 4. The undoped TiO_2 . exhibited the band gap of 3.18 eV and MNS-5 is 2.5 eV. The co-doped TiO_2 bandgap energy decreases when compared to undoped TiO_2. The extension of absorption edge towards longer wavelength (red shift) for co-doped samples indicated the decrease in band gap. This is may be due to the formation of an extra energy level above the valance band by S 2P thus the results indicated that all the co-doped samples are visible light active leads to better photocatalytic degradation efficiency by formation of photo generated electron/hole pairs.

Transmission electron microscopy (TEM) and Brauner – Emmett – Teller (BET)

TEM images of co-doped TiO_2 showed in Fig.5 (a). These results illustrated that the co-doped TiO_2 (MNS-5) nano catalysts are in spherical shape with depicts the selected area diffraction (SAED) pattern of the MNS-5, it clearly reveals well defined concentric rings which were due to the diffraction from the (101), (004), (200), (211) planes of the anatase TiO_2. The average particle size of MNS-5 was determined from the Gaussian fitting of the size histogram (Fig. 6(d)) and found to be 12.1 nm [26-27]. The surface area of co-doped TiO_2 155.78 m^2/g and pore size 4.8 nm. These results strongly confirmed that, the co-doping of Mn and S in TiO_2 lattice decreasing particle size.

The BET surface area of synthesized catalysts of undoped and co-doped (MNS-5) TiO_2 nano catalysts are 76.368 m^2/g and 155.8786 m^2/g. The pore size and volumes are given in Table.1. These results confirmed that MNS-5 showed high surface area compared to undoped TiO_2.

Evaluation of Photocatalytic Efficiency of Catalyst (MNS-5) by Degradation of Xylenol Orange (XO) dye

To obtain the optimum reaction conditions for better photocatalytic degradation of XO the effect of reaction parameters such as dopant concentration, pH, catalyst dosage and initial dye concentrations were studied by varying the desired parameter and keeping other parameters constant.

Effect of Dopant Concentration

Photocatalytic degradation of XO dye (446 nm) carried out by different synthesized catalysts with various dopant concentrations are presented in Fig.5. The co-doped (MNS-5) sample showed higher photocatalytic activity than that of undoped TiO_2 under visible light irradiation. So, it is indicated that co-doping has improved better photo catalytic performance of TiO_2. Among all the co-doped catalysts, MNS-5 showed highest percentage of degradation. This may be the dopant concentration leads to decreased band gap of TiO_2, less particle size and increased surface area of the catalyst. And also at this dopant concentration photo generated electron/hole pairs can easily transfer to the surface of catalyst by Mn and generate oxidative species such as $OH^{\bullet}$, $O_2^{\bullet -}$, $HO_2^{\bullet}$. Figure.6. indicated the apparent rates were estimated from the slopes of individual curves.

Effect of pH

Solution pH is an important variable parameter in the evaluation of photocatalytic dye degradation efficiency of the catalyst in aqueous medium because the electrostatic interactions between catalyst surface dye and charged radicals depends on the pH of the solution. Figure.7. showed that the percentage degradation of XO was carried out with MNS-5 catalyst at different pH values (2, 3, 4, 6 and 8) under visible light irradiation. From the figure it was observed that the percentage of degradation of XO is high in acidic medium compared to basic medium. This may be due to the increased electrostatic interaction between positively charged surface of the catalyst and negatively charged dye molecules. When the pH increased to basic medium the catalyst surface changes to -Ve charge and electro statically repels the same charged dye molecules. In acidic pH medium the percentage of degradation of XO was high at pH 3, at which the positive charge (H^+ ions) on TiO_2 surface increases and negatively charged XO can easily adsorbed on the catalyst surface.

Effect of Catalyst dosage

The effect of catalyst dosage on degradation of XO is given in Fig.8. The rate of degradation was carried out by varying the catalyst amounts of 100 mg/L, 150 mg/L, 200 mg/L and 250 mg/L added to 100 mL of solution containing 10 mg/L of dye at pH 3. The rate of degradation increases linearly with the increase of catalyst loading up to 100 mg/L, further increasing the catalyst dosage the degradation decreases. This may be due to increase in turbidity and agglomeration of catalyst particles which restricts the penetration of light transmission to activate the catalyst particles [28] and also collisions between active molecules and ground state molecules of co-doped TiO_2 results in deactivation of the catalyst particles [29]. Hence the optimum catalyst dosage found to be is 100 mg/L.

Effect of Initial Concentration of dye (XO)

To study the effect of initial concentration of dye (XO) at a fixed weight of catalyst dose (100 mg/L) and pH 3, the experiments were carried out with different concentrations of XO dye from 10 ppm to 40 ppm and results are presented in Fig.9. These Results demonstrate that the rate of degradation of XO dye increased upto 10 ppm. But, further increase in dye concentration causes deactivation of the catalyst due to the blanket effect and decreases the rate of degradation [30].

Antibacterial Studies

The antibacterial activity of TiO_2 nano particles were carried out by Agar-well diffusion method [31] against *Sphingomonas paucimobilis* (MTCC-6363)and different concentration of co-doped TiO_2 (MNS-5) nano particles were taken in different wells in a petri dish with a concentration ranging from 200µg/mL, 300µg/mL, 400µg/mL and chloromphenicol(control). The anti bacterial petri plates are showed in Fig .10. The bacterial growth of zone diameter values presented in Table.2.The activity results were showed that (400 µg/mL) is best concentration for the co-doped TiO_2 for the zone of inhibition of both the bacteria and also very

close to the standard values. Therefore the co-doped TiO_2 nano particles exhibiting better antibacterial activity. This inhibition may be due to the electron hole which is forms in valance band of TiO_2 by irradiation of catalyst with visible light. During the visible light this e^-/h^+ +ve hole acts as an strong oxidizing agent could degrade the protein coat of the bacteria leads to the inhibition of the growth of the organism.

CONCLUSION

Mn and S co-doped anatase TiO_2 was successfully synthesized by sol-gel method and characterised by various analytical techniques. In Mn and S co-doped TiO_2, Sulfur causes the shift in absorbance band of TiO_2 from Uv to visible region, whereas doping of Mn inhibits the electron/hole recombination and acts as charge carrier during photocatalytic degradation under visible light irradiation. 1.00 wt % Mn and 0.25 wt% S co-doped TiO_2 exhibited small particle size, high surface area gives high photoctalytic activity compared to undoped TiO_2. Finally the optimum reaction parameters were established and Xylenol orange dye, (10 ppm) was successfully degraded by 0.10g co-doped catalyst (MNS-5) at pH 3 in 120 min and also MNS-5 showed strong antibacterial activity against *Sphingomonas paucimobilis* (MTCC-6363). It may be concluded that Mn and S co-doped TiO_2 acts as better photocatalytic activity and good antibacterial agent.

Acknowledgement

I thankful to the University Grants Commission (UGC) for providing BSR fellowship.

References

1. Barka N, Bakas I, Qourzal S, Assabbane A, Ait-Ichou Y, An *inter. nation. res. journ pure .appl. chem*. 29 (2013) 1055-1060.
2. Houas A, H. Lachheb , Ksibi M, Elaloui E, Guillard C, Hermann J M, *Appl.catal.B: environ*, 31 (2001) 145-157.
3. Ioannis K, Konstantinou, Triantafyllos , Albanis A, *Appl. Catal. B: Environ*. 49 (2004) 1–14.
4. Yu D, Bai J, Liang H, Wang J, Lia C, *RSC. Adv ,* 2015.
5. Shang X L, Li C H, *Asian. Journ. Chem,* 26 (2014) 7657-7661.
6. Balkwill D L, Fredrickson J K, Romine M F "Sphingomonas and Related Genera" in M.Dworkin The Prokaryotes: An Evolving Electronic Resource for the Microbiological Community, Springer-Verlag, New York.
7. Ryan M P, Adley C C, *Journ. Hospital. Infection*, 75(2010)153-157.
8. Wang D, Yu B, Zhou F, Wang W, Liu W, *Mater. Chem. Phys,* 113 (2009) 602-606.
9. Khan S U M, Al-Shahry M, Ingler Jr W B I, *Science*. 297 (2002) 2243–2245.
10. Woo Kim K S, Kim T J , Nam C M, *Mater .Chem. Phys,* 112(2008)167-172.
11. Zeng H, Cai W, Liu P, Xu X , Zhou H , Klingshirn C , *ACS. Nano*, 2 (2008) 1661–1670.
12. Qian J , Liu P , Xiao Y , JiangY , CaoY , AiX , Yang H, *Adv. Mater*.21 (2009) 3663–3667.
13. Asahi R, Morikawa T, Ohwaki T, Aoki K, Taga Y ,*Science*.293 (2001) 269-271.
14. Zhang, Wu Y, Xing M, Leghari S A K , Sajjad S, *Energy . Environ. Sci* 3(2010) 715–726.
15. Kubacka A, ColónG , Fernández-García . *Catal . Today*, 143(2009) 286–292.
16. [16] Miguel I, Pelaez T, Nicholas T , Nolan ,environmental engineering and science program, school of energy, environmental, biological, and medical engineering, university of cincinnati, cincinnati, ohio 45221-0071,
17. Randeniya L K, Murphy A B, Plumb I C, *Journ. Mater. Sci*, 43 (2008) 1389-1399.
18. Siva Rao T, A Segne T , Susmitha T, Balaram Kiran A, Subrahmanyam C, *Adva. Mater. sci.eng*, 2012 (2012)1-9.
19. Jentys A, Pham N H, Vinek H, Englisch M , Lercher J A, *Microporous Mater,* 6 (1996) 13–17.
20. Deng Q R, Xia X H, Guo M L, Gao Y, Shao G, *Materials*, 65 (2011) 2051-2054.
21. Sang-Hun Nama, Tae Kwan Kimb, Jin-Hyo Booa, *Catal. Today*, 185 (2012)259-262.
22. Elmorsi M, Riyad Y M, Mohamed Z H and Abd Bary H M H , *J. Hazard. Mater*, 174 (2010) 352–358.
23. Sharotri N and Sud D , *Desalin. Water Treat*, (2015)1-13.
24. Sharotri N and. Sud D, *New J. Chem*, 39 (2015) 217-2223.
25. Chang S, Chien-yao H, Pin-han L , Chang-tuan , *Appl. catal B: Environ*, 90 (2009) 233-241.
26. Yoong L S, Chong F K, Dutta B K, *J. Energy*, 34(2009)1652-1661.
27. Gharibshahi L, Saion E , *Int. Journ. Mol. Sci*, 13(11) (2012) 14723-14741.
28. Chen C C, *J. Molecul .Catal. A: Chemical*, 264(2007) 82-92.
29. Kusvuran E, Gulnaz O, Irmak S, Atanur O M, Yavuz H I, Erbatur O, *J. Hazard. Mater. B*, 109(2004) 85-93.
30. *Chiou C H, Juang R S , J. Hazard. Mater*, 149 (2007) 669-678.
31. Ahmad T, Phul R , Khatoon N, Sardar M, *New J. Chem ,* 2017.
32. Synthesis of metal and nonmetal co-doped TiO_2 nano material for the improved photocatalytic and Antibacterial activity studies

How to cite this article:

Divya Lakshmi K V and Siva Rao T (2019) 'Synthesis of Metal And Nonmetal Co-Doped Tio2 Nano Material for the Improved Photocatalytic and Antibacterial Activity Studies', *International Journal of Current Advanced Research,* 08(03), pp. 17606-17611. DOI: http://dx.doi.org/10.24327/ijcar.2019.17611.3345